Targeting Oncogene mRNA Translation in B-Cell Malignancies with eFT226, a Potent and Selective Inhibitor of eIF4A

Peggy A. Thompson, Boreth Eam, Nathan P. Young, Sarah Fish, Joan Chen, Maria Barrera, Haleigh Howard, Eric Sung, Ana Parra, Jocelyn Staunton, Gary G. Chiang, Adina Gerson-Gurwitz, Christopher J. Wegerski, Andres Nevarez, Jeff Clarine, Samuel Sperry, Alan Xiang, Christian Nilewski, Garrick K. Packard, Theodore Michels, Chinh Tran, Paul A. Sprengeler, Justin T. Ernst, Siegfried H. Reich, and Kevin R. Webster

ABSTRACT

The PI3K/AKT/mTOR pathway is often activated in lymphoma through alterations in PI3K, PTEN, and B-cell receptor signaling, leading to dysregulation of eIF4A (through its regulators, eIF4B, eIF4G, and PDCD4) and the eIF4F complex. Activation of eIF4F has a direct role in tumorigenesis due to increased synthesis of oncogenes that are dependent on enhanced eIF4A RNA helicase activity for translation. eFT226, which inhibits translation of specific mRNAs by promoting eIF4A1 binding to 5′-untranslated regions (UTR) containing polypurine and/or G-quadruplex recognition motifs, shows potent antiproliferative activity and significant *in vivo* efficacy against a panel of diffuse large B-cell lymphoma (DLBCL), and Burkitt lymphoma models with ≤1 mg/kg/week intravenous administration. Evaluation of predictive markers of sensitivity or resistance has shown that activation of eIF4A, mediated by mTOR signaling, correlated with eFT226 sensitivity in *in vivo* xenograft models. Mutation of PTEN is associated with reduced apoptosis *in vitro* and diminished efficacy *in vivo* in response to eFT226. In models evaluated with PTEN loss, AKT was stimulated without a corresponding increase in mTOR activation. AKT activation leads to the degradation of PDCD4, which can alter eIF4F complex formation. The association of eFT226 activity with PTEN/PI3K/mTOR pathway regulation of mRNA translation provides a means to identify patient subsets during clinical development.

Introduction

B-cell malignancies are often associated with dysregulation of oncoproteins involved in cell proliferation and survival. Oncoprotein expression is tightly controlled at the level of mRNA translation and is largely regulated by the eukaryotic translation initiation factor 4F (eIF4F), a complex consisting of eIF4A, eIF4E, and eIF4G (1). The translation initiation factor eIF4A is a member of the "DEAD box" family of helicases that catalyze the ATP-dependent unwinding of RNA duplexes and facilitates 43S ribosome complex scanning through highly structured regions of the 5′-untranslated region (UTR) and recognition of the AUG initiation codon. The eIF4A-dependent translatome is enriched for mRNAs containing 5′-UTR polypurine and GC-rich sequence motifs with the potential to form structural elements (2). eIF4A activity is enhanced through activation of the PI3K and RAS pathways resulting in selective upregulation of oncogenes with highly structured 5′-UTRs that are involved in the proliferation, survival, and metastasis of B-cell malignancies (3–5). PI3K signaling is activated in most cancers, with PIK3CA and PTEN being the second and third most mutated cancer genes, resulting in dysregulation of eIF4A in the majority of human tumors (6). eIF4A helicase activity is tightly controlled by the cofactors eIF4B and eIF4G, whose association with eIF4A promotes processive RNA helicase activity, and programmed cell death 4 (PDCD4), a negative regulator of translation initiation that binds eIF4A preventing the formation of the eIF4F complex (7). Regulation of eIF4A through AKT and p70S6K-dependent phosphorylation of eIF4B and PDCD4, and mTOR-mediated phosphorylation of eIF4G facilitates full activation of eIF4A and formation of eIF4F (8–11). Overexpression of

eFFECTOR Therapeutics, Inc., San Diego, California.

Note: Supplementary data for this article are available at Molecular Cancer Therapeutics Online (http://mct.aacrjournals.org/).

Current address for Boreth Eam: Calporta Therapeutics, San Diego, California; current address for Nathan P. Young, Casma Therapeutics, Cambridge, Massachusetts; current address for Sarah Fish, Plexium Inc., San Diego, California; current address for Joan Chen, Certis Oncology Solutions, San Diego, California; current address for Maria Barrera, Turning Point Therapeutics, San Diego, California; current address for Haleigh Howard, Providence Portland Medical Center, Portland, Oregon; current address for Eric Sung, Fate Therapeutics, San Diego, California; current address for Ana Parra, Turning Point Therapeutics, San Diego, California; current address for Andres Nevarez, Escient Pharmaceuticals, San Diego, California; current address for Jeff Clarine, Gossamer Bio, San Diego, California; current address for Alan Xiang, WuXi AppTec, San Diego, California; current address for Christian Nilewski, Genentech Inc., South San Francisco, California; current address for Garrick K. Packard, Inception Therapeutics, San Diego, California; current address for Theodore Michels, Gossamer Bio, San Diego, California; current address for Justin T. Ernst, Inception Therapeutics, San Diego, California; current address for Siegfried H. Reich, Turning Point Therapeutics, San Diego, California; and current address for Kevin R. Webster, Frontier Medicines, San Francisco, California.

Corresponding Author: Peggy A. Thompson, Department of Cancer Biology, eFFECTOR Therapeutics, 11180 Roselle St., Ste A, San Diego, CA 92121. Phone: 858-925-8207; E-mail: pthompson@effector.com

Mol Cancer Ther 2021;20:26–36

doi: 10.1158/1535-7163.MCT-19-0973

eIF4A or the loss of PDCD4 expression has been associated with poor prognosis in multiple disease indications (2, 12). In addition, elevated eIF4B expression, a key activator of eIF4A, has been correlated with poor survival in patients with B-cell lymphoma, including DLBCL, the most common form of non-Hodgkin lymphoma (4).

In this study, we demonstrate that eFT226, a novel, potent and sequence selective inhibitor of eIF4A-dependent translation, coordinately blocks the translation of key oncogenes and survival factors in models of B-cell lymphoma. eFT226 treatment downregulates the protein expression of key transcription factors MYC and BCL6, leading to selective gene expression reprograming, inhibition of cell proliferation, and induction of cell death leading to efficacy in multiple lymphoma tumor models. Furthermore, examination of PI3K/mTOR activation status in a panel of lymphoma models has shown that the activation state of eIF4A and resultant sensitivity to eFT226 is dependent on PI3K/mTOR signaling. Interestingly, PTEN mutations stimulate AKT signaling without activating the mTOR pathway, resulting in PDCD4 degradation and resistance to eFT226. Together, these data support further evaluation of eFT226 in lymphoma and provide biomarkers for patient stratification.

Materials and Methods

Reagents

eFT226 was prepared in-house (example 231F, ref. 13), MK2206 (14), and idelalisib were purchased from Selleck Chemicals, Rocaglamide A (RocA) and cycloheximide were purchased from Sigma-Aldrich. Cell lines were purchased from ATCC (Pfeiffer, Ramos, RL, SU-DHL2, SU-DHL6), DSMZ (Carnaval, SU-DHL10), or Sigma (Karpas422). *Mycoplasma* testing or cell line authentication were not performed. From thawing, cells were recovered for two passages and then passaged a maximum of 10 times when experiments were performed. The GAPDH antibody was purchased from Santa Cruz Biotechnology. The c-MYC and p-PDCD4 S457 antibodies were purchased from Abcam. The Cyclin D1 antibody was purchased from Sigma-Aldrich. Antibodies against AKT, p-AKT T308 and S473, BCL2, BCL6, Cyclin D3, CDK4, eIF4B, p-eIF4B S422, eIF4G, p-eIF4G S1108, MCL1, PDCD4, PTEN, rpS6, p-rpS6 S235/S236 and S240/S244, p70S6K, p-p70S6K T389, and β-actin were purchased from Cell Signaling Technology. Secondary antibodies (donkey anti-rabbit IRDye-800CW, donkey anti-mouse IRDye-680RD) for Odyssey infrared imaging were purchased from LI-COR.

Cell proliferation assay

Tumor cells were cultured in RPMI media, 10% FBS, and 1× penicillin/streptomycin. Exponentially growing cells were seeded at 2,000 to 5,000 cells per well in a 96-well round bottom nontissue culture-treated plate in 90 μL growth media and cultured overnight. Cells were treated with eFT226 and the indicated compounds as single agents or in combination (fixed ratio) in an 8-point threefold dilution series. The final DMSO concentration was 0.1%. Cells were incubated for 72 hours at 37°C in a CO_2 incubator. Baseline viability of untreated cells was measured on the day of treatment and proliferation was measured after 72 hours of drug treatment using CellTiter-Glo (CTG) reagent from Promega according to the manufacturer's instructions. Calculation of CTG % Inhibition = (([inhibitor] – baseline)/(DMSO – baseline)) × 100. Drug synergism was analyzed using CalcuSyn (Biosoft) to determine combination index (CI) values, where synergy is defined as CI < 0.9, additive activity 0.9–1.1 and antagonism >1.1 (15).

Apoptosis induction assays

Exponentially growing cells were seeded at 20,000 cells per well in 96-well round bottom nontissue culture-treated plates and cultured overnight. Cells were then treated with eFT226 or DMSO for the indicated amount of time. Apoptosis and cell death were measured using BD Annexin V FITC Apoptosis Detection Kit from BD Biosciences according to the manufacturer's instructions. Briefly, cells were washed with PBS and resuspended in 1× Annexin V binding buffer containing Annexin V and propidium iodide (PI). Cells were incubated at room temperature for 15 minutes followed by dilution in Annexin V buffer. Fluorescence of the cells was analyzed by flow cytometry using Attune NxT flow cytometer Thermo Fisher Scientific.

Preparation of lysates and Western blot analysis

Cells untreated or treated with DMSO, eFT226, idelalisib, or MK2206 for the indicated time were pelleted by centrifugation, washed once with ice-cold PBS, and lysed in 1× Cell Lysis Buffer (Cell Signaling Technology) supplemented with a final concentration of 1 mmol/L PMSF. Protein concentrations in cell lysates were quantitated by BCA protein assay (Thermo Fisher Scientific). Lysates were analyzed on the Wes Simple Western system (total and phosphor-eIF4G) according to the manufacturer's instructions or equal amounts of total protein were resolved by SDS-PAGE, immunoblotted with the indicated antibodies, and visualized by LI-COR Odyssey imager (LI-COR).

Generation of PTEN KO cell line

Pfeiffer cells were infected via spin-fection with concentrated MSCV-Cas9-EF1a-GFP viral particles (CASLV125VA-1, SBI Biosciences). GFP^+ cells were then FAC-sorted by flow cytometry (Flow Cytometry facility, SBP Medical Discovery Institute). The polyclonal population of high GFP^+ cells were infected with EF1a-RFP-U6-gRNA lentivirus (CASLV512PA-R, SBI Biosciences) containing either control gRNA (GTATTACTGATATTGGTGGG) or *PTEN* gRNA (ACGCCTTCAAGTCTTTCTGC). gRNAs were cloned into the vectors and virus was generated according to the manufacturer's instructions. GFP^+/RFP^+ cells were FAC-sorted by flow cytometry. Single cell–derived clones were expanded and individually tested for PTEN knockout by Western blot analysis. Control and PTEN knockout cells were treated with eFT226, RocA, or DMSO for 48 hours. Caspase-3/7 activation was detected using CaspaseGlo reagent (Promega) and normalized to the number of live cells using the CTG luminescent assay (Promega).

In vivo studies

All animal studies were carried out in accordance with the guidelines established by the Institutional Animal Care and Use Committee at Explora BioLabs (ACUP# EB17-010-033) or Crown Biosciences. For subcutaneous xenograft studies, mice (4- to 8-week-old females, 16–24 g) were implanted with an equal volume (1:1) ratio of tumor cells and Matrigel (BD Biosciences) for tumor development. When the mean tumor size reached approximately 110 to 150 mm^3, the mice were randomized and size-matched into vehicle and treatment groups. Tumor size was measured in length and width with a caliper twice a week. The tumor volume was calculated by the formula $L \times W \times W/2$ according to NCI standards. Body weights were collected prior to study start and twice a week during the study. eFT226 was formulated in 5% dextrose in water (D5W) and immediately dissolved into solution. Subcutaneous studies: [TMD8 5×10^6 cells in NOD.SCID (Charles River Laboratories), mean tumor initiation size 150 mm^3; Pfeiffer 1×10^7 cells in NOD.SCID, mean tumor initiation size 190 mm^3;

Carnaval 5×10^6 cells in NOD.SCID, mean tumor initiation size 145 mm^3; SU-DHL10 1×10^7 cells in NOD.SCID, mean tumor initiation size 113 mm^3; RL 1×10^7 cells in NOD.SCID, mean tumor initiation size 110 mm^3; Karpas422 1×10^7 cells in NOD.SCID, mean tumor initiation size 150 mm^3; SU-DHL2 1×10^7 cells in BALB/c nude, mean tumor initiation size 110 mm^3].

For orthotopic xenograft studies, 50 mg tumor fragments were implanted into the left renal capsule and dosing was initiated 3 days postsurgery: [HBL-1 NOD.SCID; SU-DHL6 CB17 SCID (Charles River Laboratories); Ramos NOD.SCID]. Mice were randomized according to original tumor fragment size and assigned into vehicle and treatment groups. At the end of the treatment period, both the right and tumor-implanted left kidneys were excised and weighed. Tumor weight was calculated by subtracting the weight of the right kidney from the weight of the tumor-implanted left kidney in the same animal.

For pharmacodynamic (PD) studies, tumors were excised from animals and snap frozen in liquid nitrogen. Frozen tumor was weighed out and 6x (volume:tumor weight) of 1× Cell Lysis Buffer supplemented with protease and phosphatase inhibitors (Sigma) was added to the sample in a Lysing Matrix A Tube (Thermo Fisher Scientific). Samples were homogenized using a Precellys24 homogenizer (Bertin Technologies) and lysates were clarified by centrifugation. Protein concentrations in cell lysates were quantitated by BCA protein assay and equal amounts of total protein were resolved by SDS-PAGE, immunoblotted with the indicated antibodies, and visualized by LI-COR Odyssey imager.

To determine tumor drug levels, tumor samples were diluted with water, homogenized, and added directly into a Strata Impact protein precipitation plate (Phenomenex) containing acetonitrile with an internal standard. Samples were vortexed and filtered directly into a 96-well polypropylene plate and subjected to bioanalysis. Tissue standards were prepared by spiking into blank matrix and serially diluting eFT226 to obtain a standard calibration range. Tumor tissue preparations were analyzed by LC-MS.

Results

eFT226 is a potent inhibitor of oncogenic drivers of B-cell malignancies

The PI3K/AKT/mTOR signaling pathway plays an important role in controlling proliferation and survival of tumor cells, including B-cell lymphomas. Activation of PI3K/AKT/mTORC1 causes increased mRNA translation, protein synthesis, and cellular proliferation partly by activation of eIF4A through phosphorylation of eIF4G, eIF4B, and PDCD4 (**Fig. 1A**). AKT and p70S6K have been shown to directly phosphorylate the eIF4A regulators PDCD4 (S67 and S457) and eIF4B (S422) (refs. 11, 16, 17), whereas mTOR has been reported to phosphorylate eIF4G (S1108), the scaffolding protein that regulates eIF4A binding and eIF4F complex formation (9). The PI3K/AKT/mTOR pathway is reported to be dysregulated in B-cell lymphoma and drives the overexpression of oncogenes and survival factors including MYC, CDK4, Cyclin D1/3, BCL2, and MCL1. These mRNAs contain sequence motifs that promote highly structured 5′-UTRs resulting in a greater dependence on enhanced eIF4A RNA helicase activity to drive mRNA oncogene translation (4, 18–20).

Biochemical analysis shows that eFT226 (**Fig. 1B**; ref. 21) is a potent and RNA sequence selective inhibitor of eIF4A1-dependent translation that promotes eIF4A1 binding to specific 5′-UTR polypurine recognition motifs similar to RocA (22). This results in the formation of a stable ternary complex that leads to a selective block in ribosome mRNA scanning. Introduction of the F163L mutation into the rocaglamide binding site in eIF4A1 prevented eFT226 binding to eIF4A1 and rescued eFT226 antiproliferative activity (21) consistent with what has been reported for Silvestrol and RocA (23–25). Genome-wide ribosome profiling of eFT226 in the activated B-cell (ABC) DLBCL TMD8 cell line confirmed that select genes were translationally downregulated and contained 5′-UTR polypurine and G-quadruplex-like recognition motifs (Supplementary Table S1; Supplementary Fig. S1A), similar to what has been reported for other eIF4A inhibitors (22, 25–27). Target genes with reduced ribosome footprint density with eFT226 treatment *MYC, CCND1, BCL2, CDK4*, and *CARD11* (Supplementary Fig. S1B) and have been reported to be sensitive to eIF4A inhibition (19, 20, 26–28). Polysome profile analysis of TMD8 cells treated with eFT226 confirmed translational repression of eFT226-sensitive target genes (e.g., *MYC, CCND1, BCL2, MCL1*, and *CDK4*), whereas housekeeping genes were unchanged with eFT226 treatment (Supplementary Fig. S1C and S1D).

To confirm that translational regulation by eFT226 of key oncogenic drivers is mediated through the 5′-UTR, cell lines were generated with doxycycline-inducible gene constructs that expressed *MYC* or *MCL1* mRNA with (wt UTR) or without 5′-UTR (ΔUTR) sequences in HEK293T cells. Deletion of the normal 5′-UTR sequences (ΔUTR) rendered *MYC* or *MCL1* gene expression resistant to eFT226, whereas expression of *MYC* or *MCL1* under the control of its natural 5′-UTR (wt UTR) retained sensitivity to eFT226 (Supplementary Fig. S2). These results further support that eFT226 translationally regulates its target genes through recognition elements within the 5′-UTR (21).

Translational regulation of key oncogenic drivers of lymphoma suggested that eFT226 could be efficacious in B-cell malignancies. Therefore, eFT226 was tested against a panel of B-cell tumor cell lines that included DLBCL, Burkitt lymphoma, multiple myeloma, mantle cell lymphoma, and Hodgkin lymphoma. eFT226 treatment resulted in potent and differential inhibition of proliferation across cell lines (mean $GI_{50} = 9$ nmol/L) with increased sensitivity observed within the DLBCL subtype (**Fig. 1C**). Consistent with eFT226′s mechanism of action, treatment of lymphoma cell lines with eFT226 resulted in potent downregulation of MYC, Cyclin D1/3, BCL6, or MCL1 protein levels in ABC DLBCL (TMD8 and HBL1), germinal center B-cell (GCB) DLBCL (Pfeiffer, SU-DHL6, SU-DHL10, RL, and Karpas422), and Burkitt lymphoma (Ramos) cell lines, whereas the expression level of housekeeping genes (i.e., GAPDH and/or β-actin) was unchanged (see **Fig. 1D** and Supplementary Fig. S3A). Cell-cycle analysis showed that incubation with eFT226 resulted in an increase in the percentage of cells in the G_1 phase and a corresponding decrease in the S-phase cells in multiple cell lines (Supplementary Fig. S3B–S3E). A block in G_1 progression by eFT226 is consistent with downregulation of CDK4, cyclin D1 or D3 as well as MYC and MYC target genes implicated in cell-cycle progression.

Recognizing that key transcription factors (MYC and BCL6) essential for lymphoma development were selectively downregulated at the protein level by eFT226, the ability of the drug to reshape the tumor cells transcriptional program was assessed. A global transcript RNA sequencing (RNA-Seq) analysis was conducted in TMD8 cells treated with either eFT226 or DMSO control for 6 hours. Global expression analysis using IPA software predicted the inhibition of key transcription factors MYC and BCL6 (Supplementary Table S1), confirming a functional consequence of inhibition by eFT226. GSEA analysis of the RNA-Seq dataset using the molecular signatures database (MsigDB) identified the Schuhmacher_MYC_Targets

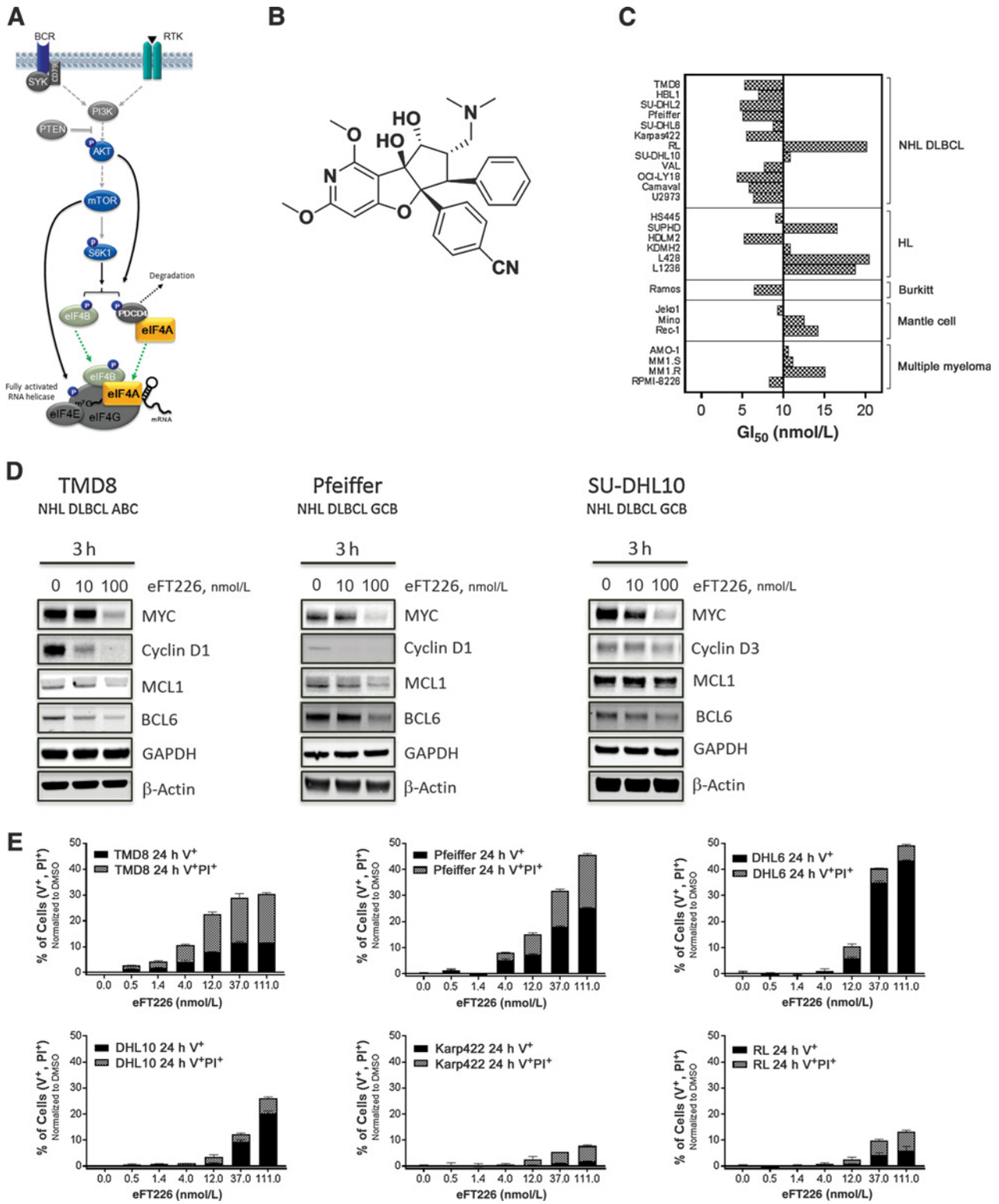

Figure 1.

eFT226 is active against a panel of B-cell tumor cell lines. **A,** Schematic of PI3K/AKT/mTOR pathway activation of eIF4A regulators. **B,** Chemical structure of eFT226 (21). **C,** Tumor cell lines were incubated with various concentrations of eFT226 for 72 hours, and cell proliferation was assessed by the CellTiter Glo assay. Mean GI_{50} was determined to be 9 nmol/L. **D,** Immunoblots demonstrate that eFT226 inhibition of eIF4A decreases protein expression of MYC, Cyclin D1/3, MCL1, and BCL6 in TMD8, Pfeiffer, and SU-DHL10 lymphoma cell lines. **E,** Incubation of tumor cells with increasing concentrations of eFT226 for 24 hours was analyzed by Annexin (V^+) and PI flow cytometry. A dose-dependent increase in cells undergoing apoptosis (V^+) and cell death (V^+ PI^+) was observed with eFT226 treatment. PTEN wt: TMD8, Pfeiffer, and SU-DHL6; PTEN mutant: SU-DHL10, Karpas422, and RL.

MYC signature among the most significantly enriched for eFT226 treatment compared with DMSO control (Supplementary Fig. S1E). Identification of transcription factor signatures consistent with the downregulation of protein levels for MYC and BCL6 with eFT226 treatment suggests the ability for selective transcriptional reprograming in lymphoma cell lines.

The BCL2 family proteins MCL1 and BCL2 are important regulators of apoptosis. These corresponding transcripts have been reported to contain long 5′-UTR regions and high G/C content resulting in complex hairpin structures that require eIF4A helicase activity for efficient scanning of the 40S ribosomal subunit and are more dependent on the eIF4F complex for translation (18). Evaluation of MCL1 or BCL2 protein levels by Western blot analysis showed that eFT226 treatment caused a reduction in MCL1 protein levels as early as 3 hours and essentially complete loss of MCL1 protein by 24 hours. Regulation of BCL2 was only observed with 24-hour drug treatment (Supplementary Fig. S3A). MCL1 protein is known to have a much shorter half-life than BCL2 (<1 hour compared with 16–24 hours) consistent with the differential time dependent regulation of these target proteins by eFT226 (29, 30).

The effect of eFT226 on tumor cell survival was evaluated by monitoring apoptosis and cell death markers during drug treatment. Lymphoma cell lines were treated with increasing concentrations of eFT226 and stained with Annexin V (indicative of early apoptosis) and PI (indicative of cell death). eFT226 potently induced apoptosis (Annexin V^+, PI^- stained cells) and/or cell death in ABC-DLBCL (TMD8) and GCB-DLBCL (Pfeiffer and SU-DHL6) lymphoma cell lines with approximately 10% to 50% apoptosis and/or cell death observed within 24 hours of drug treatment (**Fig. 1E**). This apoptotic signature is consistent with an eFT226-dependent rapid and potent downregulation of MCL1 protein levels. At equivalent concentrations of eFT226, GCB-DLBCL cell lines containing PTEN mutations (Karpas422, RL, and SU-DHL10) exhibited substantially reduced Annexin V^+ or PI^+ staining (**Fig. 1E**). These results suggest that the differential effects of eFT226 on tumor cell survival corresponds with alterations in PTEN.

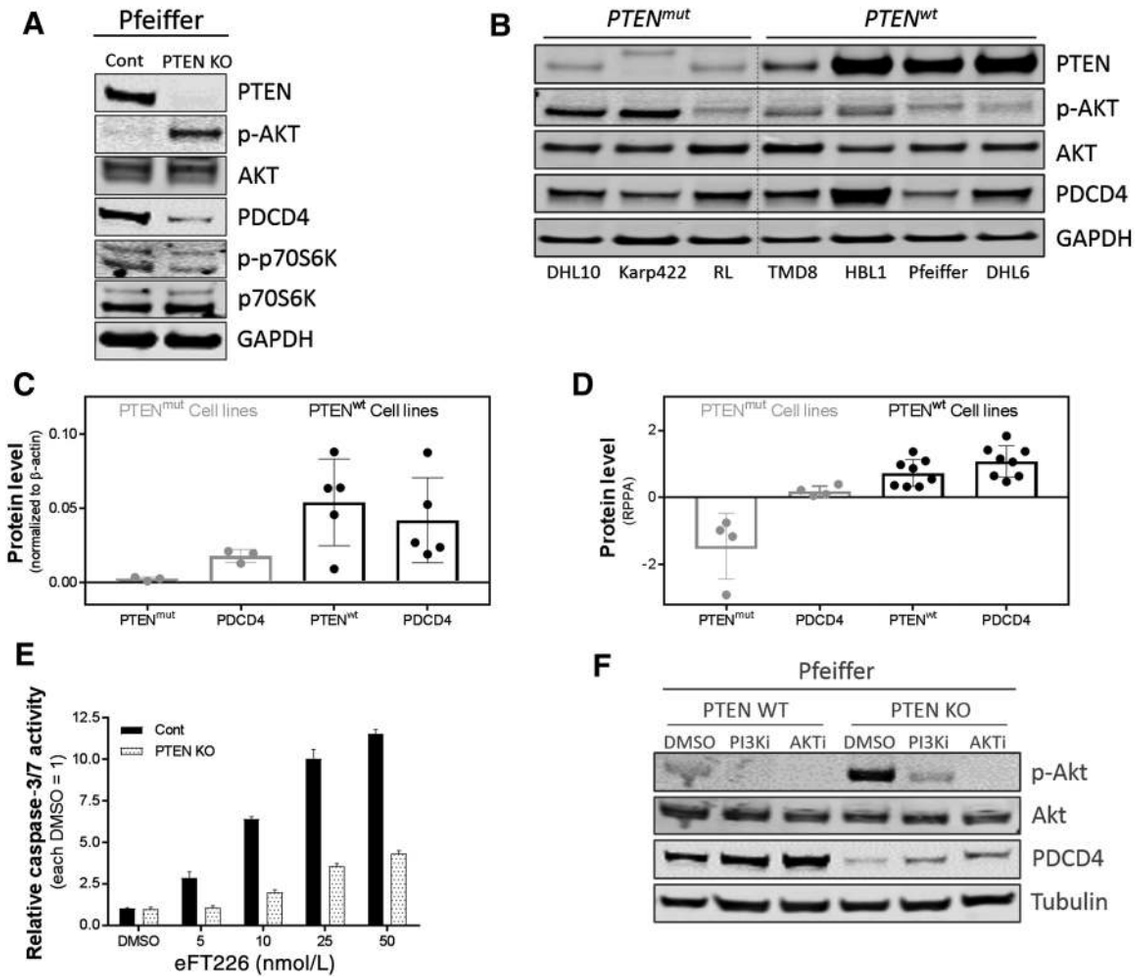

Figure 2.

PTEN loss decreases sensitivity to eFT226 in lymphoma cell lines. **A,** The PTEN gene was knocked out using CRISPR gene editing in Pfeiffer cells resulting in increased p-AKT S473 and decreased PDCD4 as measured by immunoblot analysis. **B,** Evaluation of PTEN status and AKT signaling in lymphoma cell lines. **C** and **D,** Correlation of PTEN and PDCD4 protein levels in DLBCL cell lines determined by immunoblot analysis (**C**) and DLBCL cell lines within the CCLE RPPA database (**D**). **E,** Knockout of PTEN in the Pfeiffer cell line results in decreased sensitivity to induction of apoptosis with eFT226 treatment. **F,** Treatment of the Pfeiffer wt and PTEN KO cell lines with 1 μmol/L PI3K/AKT inhibitors (idelalisib and MK2206) for 4 hours inhibit AKT signaling resulting in an increase in PDCD4 protein levels.

PTEN loss reduces sensitivity to eFT226

To further test the dependency of eFT226 sensitivity on PTEN status, CRISPR gene editing technology was used to knockout PTEN in the Pfeiffer GCB-DLBCL cell line. As shown in **Fig. 2A**, loss of PTEN resulted in activation of AKT signaling, as seen by an increase in AKT S473 phosphorylation, as well as a reduction in PDCD4 protein levels. Surprisingly increased AKT signaling did not result in activation of mTOR (no corresponding increase in p-p70S6K or p-eIF4G). These findings are similar to what was observed for the panel of PTEN mutant lymphoma cell lines (**Fig. 2B**; Supplementary Fig. S4A) and suggested that PTEN regulates changes in PDCD4 protein levels through activation of AKT. Comparison of PTEN and PDCD4 protein levels in the DLBCL lymphoma cell lines by western blot analysis (**Fig. 2C**) and by RPPA CCLE DLBCL cell line data analysis (**Fig. 2D**) showed a correlation between PTEN and PDCD4 protein levels. PTEN mutant cell lines corresponded with a loss of PTEN protein as well as decreased PDCD4 levels. This is consistent with cell lines containing PTEN mutations activating AKT signaling and promoting the ubiquitination and degradation of PDCD4 (10).

The Pfeiffer PTEN knockout cell line was tested for sensitivity to eFT226 and the chemical analogue RocA. Decreased induction of apoptosis was observed upon treatment with either eFT226 (**Fig. 2E**) or RocA (Supplementary Fig. S4B). This resistance to eIF4A inhibition is consistent to that seen in the $PTEN^{mut}$ lymphoma cell lines treated with eFT226 (**Fig. 1E**). We hypothesize that PTEN alterations increase AKT signaling and trigger PDCD4 degradation thereby altering the stoichiometry of eIF4A binding to PDCD4 and increasing the available levels of eIF4A to form the eIF4F complex. Increased eIF4A availability may result in higher drug levels required for inhibition. It is also possible that activation of AKT stimulates additional survival pathways that increase resistance to eFT226.

The observation that loss of PTEN function and subsequent activation of AKT decreased sensitivity to eFT226 suggests that combination of eFT226 with targeted agents that inhibit AKT signaling could be beneficial. Treatment of the Pfeiffer PTEN KO cell line with Idelalisib (PI3Ki) or MK2206 (AKTi) inhibited AKT phosphorylation and resulted in an increase in PDCD4 protein levels (**Fig. 2F**) further supporting that this combination strategy could be advantageous. Therefore, the antiproliferative activity of eFT226 was assessed in combination with Idelalisib or MK2206, in DLBCL cell lines with PTEN mutations and activated AKT signaling (SU-DHL10 and Karpas422) or the PTEN wt cell line (TMD8). CI values were calculated for each drug combination and cell line using CalcuSyn where synergy is defined as CI < 0.9, additive activity 0.9–1.1 and antagonism >1.1 (15). Combination of eFT226 with either idelalisib or MK2206 was synergistic in both the SU-DHL10 (CI of 0.54 and 0.56, respectively) and Karpas422 (CI of 0.28 and 0.51, respectively) cell lines with PTEN mutations and additive (CI of 1.1 for MK2206) in the TMD8 $PTEN^{wt}$ cell line (Supplementary Table S2) consistent with the hypothesis that hyperactive AKT signaling decreases sensitivity to eFT226. These results highlight the benefits of combining eFT226 with PI3K/AKT pathway inhibitors.

eFT226 exhibits differential *in vivo* activity across lymphoma models

The antitumor efficacy of eFT226 was assessed across a panel of lymphoma xenograft models including DLBCL (ABC and GCB) and Burkitt lymphoma (**Table 1**). Human tumor xenografts were grown in immune compromised mice and treated with eFT226 or vehicle administered intravenously on a weekly (once weekly) schedule. Treatment with 1 mg/kg eFT226 resulted in substantial tumor growth inhibition (97% and 87%) for ABC-DLBCL models TMD8 and HBL1, respectively (**Fig. 3A**; Supplementary Fig. S5G), that harbor CD79B and MYD88 activating mutations. eFT226 treatment of the TMD8 tumor model at 1 and 0.2 mg/kg once weekly resulted in dose-dependent tumor growth inhibition of 97% and 80%, respectively, at the end of the 15-day dosing period (**Fig. 3A**). eFT226 was well tolerated at all doses as seen by a lack of body weight loss (Supplementary Fig. S5A). Histopathology and IHC were performed on both vehicle and eFT226 (1 mg/kg once weekly) treated tumors on day 15. Treatment with eFT226 resulted in highly necrotic tumor tissue, downregulation of MYC, as well as increased cleaved caspase-3 indicative of ongoing apoptosis (**Fig. 3B** and **C**). Downregulation of eFT226 target genes were analyzed following administration of eFT226 in the TMD8 tumor model. Consistent with what was observed for eFT226 treatment *in vitro*, levels of MYC, Cyclin D1, MCL1, CDK4, and BCL6 protein were downregulated at 24 hours following a 1 mg/kg dose. Decreased expression of MCL1, CDK4, and BCL6 was also observed 24 hours following a dose of 0.1 mg/kg eFT226 (**Fig. 3D** and **E**).

Significant tumor growth inhibition (70% and 83%) was also observed for GCB-DLBCL tumor models Pfeiffer and SU-DHL6, respectively (**Fig. 4A**; Supplementary Fig. S5C). Inhibition of Pfeiffer tumor growth was dose dependent with efficacy observed over a 10-fold dose range (0.1–1 mg/kg; **Fig. 4A**). eFT226 was well tolerated at all doses as seen by a lack of body weight loss (Supplementary Fig. S5B). Biomarkers were further analyzed for a pharmacodynamic response at

Table 1. Antitumor activity of eFT226 in the treatment of lymphoma xenograft models.

Xenograft	Tumor type	Genomic markers	Pathway activation status	%TGI (day 15) eFT226 1 mg/kg Q1W IV	*P*
TMD8	DLBCL ABC	CD79, MYD88	mTOR high	97	<0.0005
HBL1	DLBCL ABC	CD79, MYD88	mTOR high	87	<0.0005
SU-DHL2	DLBCL ABC	CARD11, A20	mTOR low	−41	0.188
Pfeiffer	DLBCL GCB	EZH2, PIK3C2G, STAT3, SYK, BCL2 trans	mTOR high	70	<0.0005
SU-DHL6	DLBCL GCB	EZH2, PIK3C2G, TP53, BCL2 trans	mTOR high	83	<0.0005
RL	DLBCL GCB	PTEN, EZH2, BCL2 trans	PTEN	23	0.1817
Karpas422	DLBCL GCB	PTEN, EZH2, BCL2 trans	PTEN	17	0.507
SU-DHL10	DLBCL GCB	PTEN, EZH2, PIK3C2A, TP53, MYC and BCL2 trans	PTEN	37	0.0638
Carnaval	DLBCL GCB	MYC and BCL2 trans	mTOR low	37	0.0055
Ramos	Burkitt	MYC trans, TP53	mTOR high	75	<0.0005

Abbreviation: Q1W, once weekly.

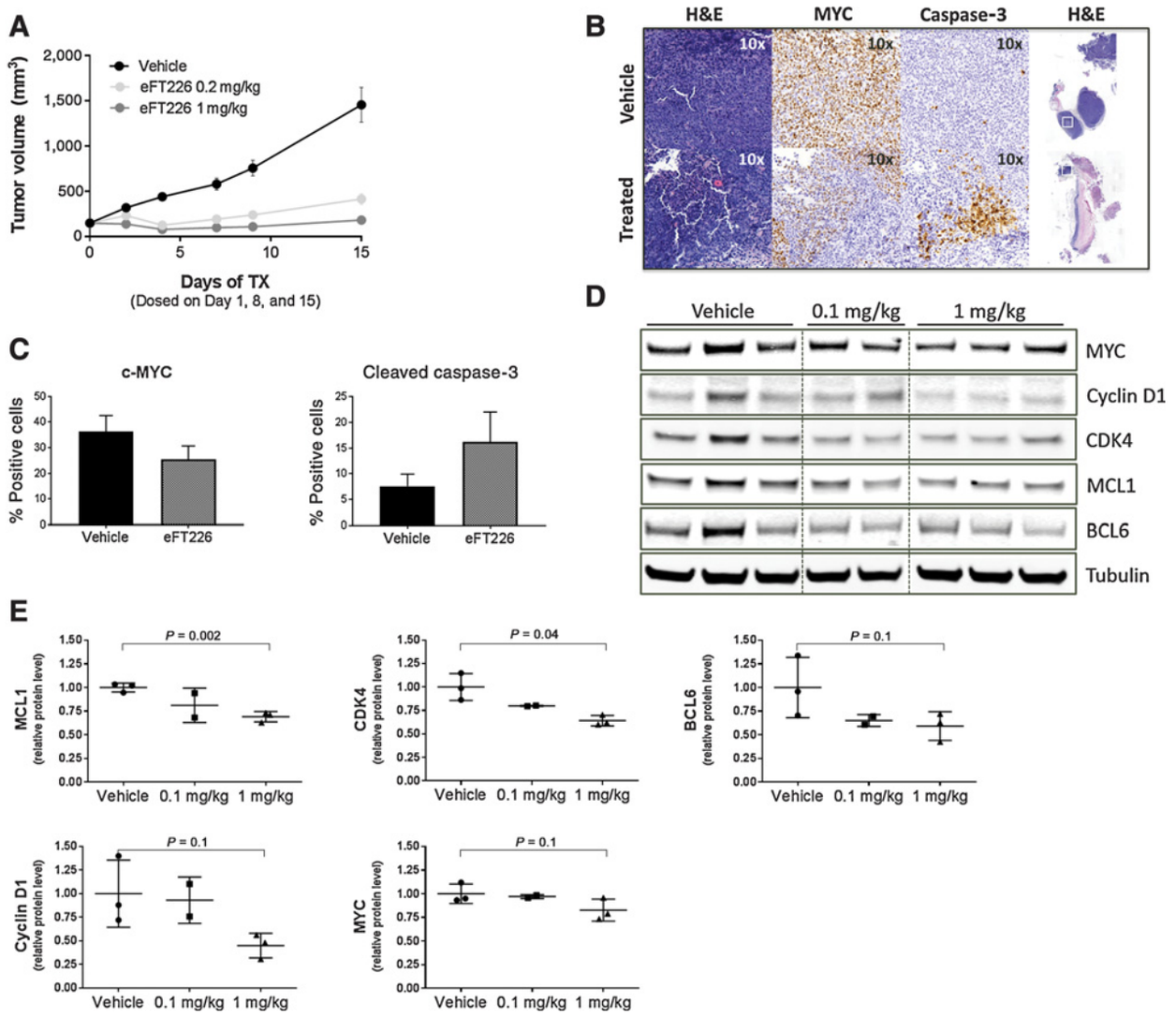

Figure 3.

eFT226 efficacy and biomarker analysis in an ABC-DLBCL xenograft model. **A,** NOD SCID mice implanted subcutaneously with TMD8 cells were treated once weekly (Q1W) with either vehicle (black) or eFT226 intravenously (1 mg/kg, dark gray; 0.2 mg/kg, light gray) for 15 days to assess the effect on tumor growth. Data shown are the average SEM. **B,** IHC analysis of TMD8 tumor 3 hours after treatment with vehicle or eFT226 (1 mg/kg once weekly) on day 15. **C,** Drug treatment downregulates MYC and induces apoptosis as seen by an increase in cleaved caspase. **D,** Immunoblot analysis of TMD8 tumors from mice 24 hours after dosing with 0.1 or 1 mg/kg eFT226. **E,** Biomarker analysis of MYC, Cyclin D1, MCL1, BCL6, and CDK4 protein levels relative to GAPDH measured 24 hours after the indicated dose of eFT226.

times ranging from 1 to 72 hours postdose. Tumor samples were collected at various time points to determine the corresponding drug levels. Following a single dose of 1 mg/kg eFT226, inhibition of MYC, Cyclin D1, and BCL6 were both time- and exposure-dependent (**Fig. 4B** and **C**). The recovery of biomarker inhibition was consistent with the clearance of eFT226 out of the tumor with protein expression returning to approximately 60% to 80% of vehicle at 24 hours. To determine the PK–PD relationship, inhibition of Cyclin D1 protein levels were quantified and eFT226 drug levels were measured. Dose proportional inhibition of Cyclin D1 was observed (**Fig. 4D**). Similarly, analysis of SU-DHL6 or Ramos tumors treated with 1 mg/kg Q1W eFT226 resulted in significant tumor growth inhibition and biomarker downregulation *in vivo* concordant with what was observed *in vitro* (see Supplementary Figs. S3A, S5C–S5F).

Identification of biomarkers that correlate with sensitivity or resistance to eFT226

Although eFT226 exhibited *in vivo* activity in models of DLBCL (ABC, GCB) and Burkitt lymphomas, it did not inhibit the tumor growth in all models even though eFT226 downregulated key drivers of tumorigenesis (i.e., MYC, Cyclin D, and BCL6) *in vitro*. We were interested in further defining drivers of sensitivity and resistance to identify patient subsets during clinical development. Activation of the PI3K/AKT/mTOR pathway in lymphoma models reportedly leads to dysregulation of eIF4A and the eIF4F complex.

Evaluation of PI3K/AKT pathway mutations across the lymphoma cell lines tested in xenograft models demonstrated that those with PTEN mutations are associated with reduced *in vivo* efficacy (**Table 1**; Supplementary Fig. S5J–S5L). This is consistent with the reduced

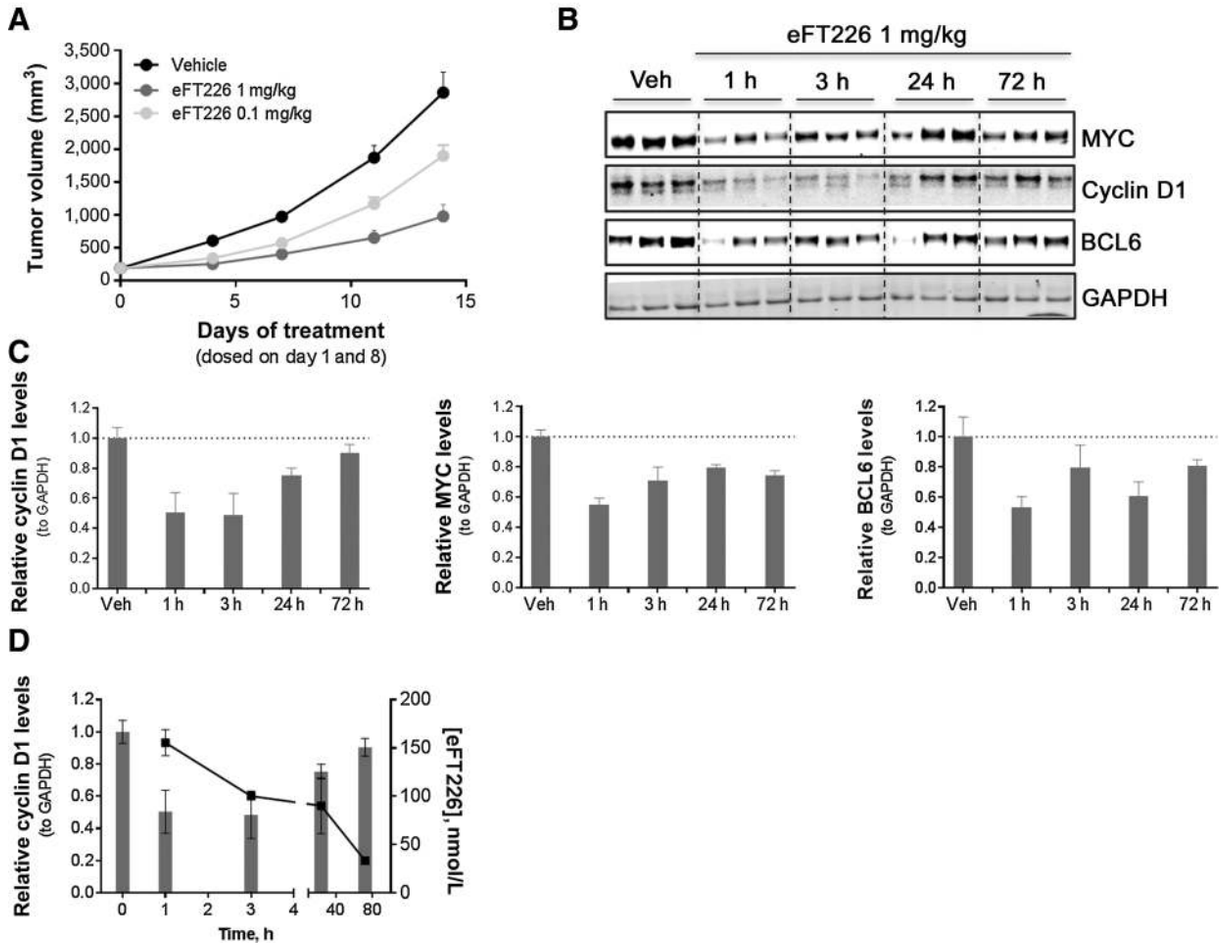

Figure 4.

eFT226 efficacy and biomarker analysis in a GCB-DLBCL xenograft model. **A,** NOD SCID mice implanted subcutaneously with Pfeiffer cells were treated once weekly (Q1W) with either vehicle (black) or eFT226 IV (1 mg/kg, dark gray; 0.1 mg/kg, light gray) for 14 days to assess effect on tumor growth. Data shown are the average SEM. **B,** Immunoblot analysis of Pfeiffer tumors for various time points from mice treated with a single 1 mg/kg dose of eFT226. **C,** MYC, Cyclin D1, and BCL6 protein levels relative to GAPDH measured at the indicated times after a single dose of eFT226. **D,** Cyclin D1 protein levels at multiple tumor drug levels were measured to determine the PK–PD relationship.

sensitivity to induction of apoptosis upon treatment with eFT226 observed *in vitro* for PTEN-mutant cell lines (**Fig. 1E**). These results seemed counterintuitive since it is expected that alterations in PTEN, a key activator of AKT signaling, would lead to increased AKT and mTOR signaling and activation of the eIF4F complex. Interestingly, even though PTEN alterations did result in activation of AKT signaling, this did not lead to an increase in mTOR signaling as evident by low phospho-to-total levels of mTOR substrates (p70S6K and eIF4G; Supplementary Fig. S4A). The association of PTEN status with eFT226 efficacy provides a genetic marker that may be useful in the analysis of patient subsets during clinical development.

PTEN status alone does not account for the pattern of differential *in vivo* activity observed across the lymphoma models, suggesting there are additional drivers of sensitivity and resistance. To determine whether mTOR signaling resulted in differential activation of eIF4A in the sensitive versus refractory ABC DLBCL tumor models, activation of the AKT/mTOR signaling pathway was assessed for these cell lines by monitoring the phosphorylation levels of mTOR substrates and eIF4A regulators. eFT226 treatment resulted in significant tumor growth inhibition (87%–97% TGI) for the TMD8 and HBL1 tumor models but no tumor growth inhibition for SU-DHL2 (see **Table 1**; Supplementary Fig. S5H). Evaluation of mTOR signaling by Western blot analysis showed that the mTOR pathway was activated in both TMD8 and HBL1 cell lines as seen by high phospho-to-total protein levels for p70S6K (T389), rpS6 (S240/244), eIF4B (S422), and eIF4G (S1108). In contrast, mTOR signaling was much lower in the SU-DHL2 cell line, suggesting that eIF4A is much less activated and corresponds to poor *in vivo* activity with eFT226 treatment (**Fig. 5A** and **B**).

mTOR pathway activation was further evaluated across the broad panel of lymphoma cell lines tested and compared with the *in vivo* sensitivity of eFT226 at a dose and schedule of 1 mg/kg once weekly. Tumor models in which eFT226 treatment yielded >60% TGI were categorized as sensitive. The 60% TGI cutoff in preclinical models has been defined by the NCI to increase the likelihood of eliciting a clinical response (31). Activation of the mTOR pathway, as evident by an

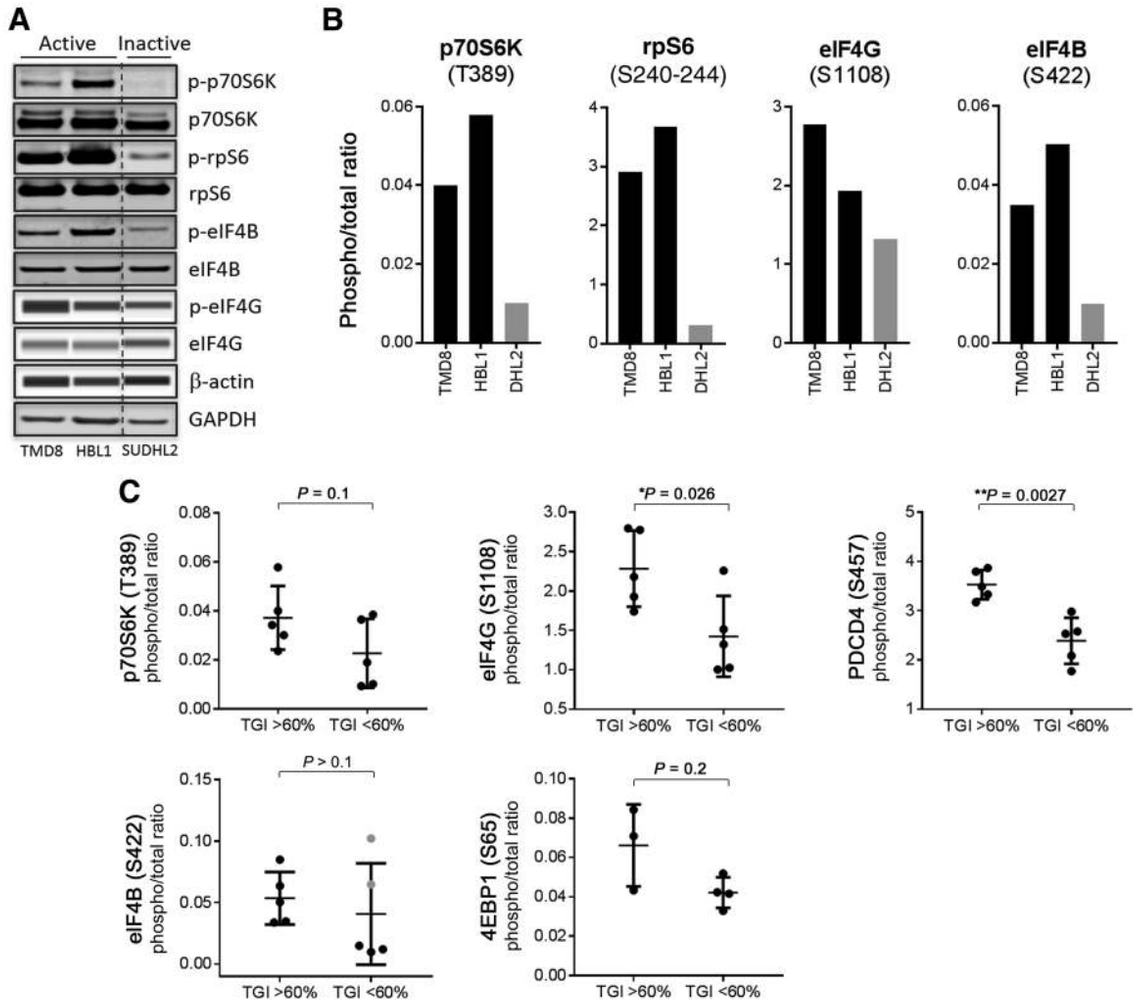

Figure 5.

PI3K/mTOR pathway activation of eIF4A is associated with increased eFT226 activity *in vivo*. **A,** PI3K/AKT/mTOR pathway activation for the ABC DLBCL cell lines assessed by Western blot analysis. **B,** Phospho/total ratio of p70S6K, rpS6, eIF4G, and eIF4B for eFT226-sensitive and -resistant ABC DLBCL lymphoma tumor models. **C,** Phospho/total ratio of p70S6K, eIF4G, PDCD4, 4EBP1, and eIF4B for eFT226-sensitive and -resistant lymphoma tumor models. PTEN-mutant models with activated AKT signaling are highlighted in gray in the eIF4B plot. 4EBP1 is not expressed in the Pfeiffer GCB DLBCL cell line.

increase in phosphorylation of p70S6K (T389), eIF4G (S1108), 4EBP1 (S65), and PDCD4 (S457) (**Fig. 5C**; Supplementary Fig. S4A), showed the greatest correlation with *in vivo* tumor growth inhibition by eFT226. The phosphorylation status of eIF4B (S422) also correlated with eFT226 sensitivity except for cell lines having a PTEN mutation where hyperactivated AKT drives increased phospho-eIF4B (**Fig. 5C**; Supplementary Fig. S4A). Interestingly, AKT signaling did not stimulate the phosphorylation of PDCD4 S457, suggesting that phosphorylation of this site is more dependent on p70S6K activation in these cell lines. This analysis suggests that collective activation of eIF4A regulators lead to enhanced eFT226 activity and provides potential tumor biomarkers to evaluate in relation to clinical activity.

Discussion

eFT226 is a potent and selective inhibitor of eIF4A-dependent translation that inhibits cell proliferation and rapidly induces cell death in B-cell lymphoma cell lines. Therapeutic benefit of eIF4A inhibition by eFT226 is mediated in part by a coordinated decrease in the protein levels of short lived oncoproteins including MYC, Cyclin D1, and MCL1, which are drivers of B-cell proliferation and survival. This results in significant antitumor activity *in vivo* across a diverse set of lymphoma xenograft models including DLBCL (ABC and GCB) and Burkitt lymphoma.

Using a genome-wide profiling approach, we identified that eFT226 translationally regulates a set of key oncogenes (e.g., MYC, Cyclin D1, CDK4, MCL1, and BCL2) that are important for B-cell tumor disease progression. The set of mRNAs regulated by eFT226 were enriched for oncogenes encoding specific polypurine and/or G-quadraplex sequences. Regulation was determined to be dependent upon sequences within the 5′-UTR and is mediated through the formation of a stable ternary complex with eIF4A, eFT226 and mRNA recognition elements that block ribosome scanning (21, 22, 25). Treatment of lymphoma tumor cells with eFT226 promotes a coordinated

translational inhibition of oncogenic drivers (MYC, Cyclin D1, CDK4, MCL1, and BCL2) and transcription factors (MYC and BCL6) that not only results in selective transcriptional reprogramming but also inhibition of proliferation and cell death.

B-cell malignancies are often associated with aberrant activation of oncogenic signaling pathways (PI3K/AKT/mTOR) that cause dysregulated protein translation (3–4). Elevated mTOR pathway activity has emerged as a major marker for aggressive disease and poor prognosis in non-Hodgkin lymphoma. Activation of cap-dependent translation via regulation of key regulators of eIF4A (eIF4G, eIF4B, and PDCD4) and the eIF4F complex is a critical output of these signaling pathways and leads to increased eIF4A activity and enhanced translation of mRNAs with highly structured 5′-UTRs (3–5). Lymphoma models with activated eIF4A, as seen by an increased phosphorylation of mTOR substrates (eIF4G and p70S6K) and eIF4A regulators (eIF4B and PDCD4), correlated with eFT226 sensitivity in *in vivo* xenograft models. Consequently, pharmacologic inhibition of the translation initiation factor eIF4A in B-cell lymphoma models with activated eIF4A is shown here to be highly effective.

Lymphoma tumor models with PTEN mutations and activated AKT signaling were less sensitive to eFT226 treatment as seen by reduced apoptosis *in vitro* and diminished *in vivo* efficacy. Interestingly, activated AKT signaling did not translate into activation of the mTOR pathway and presumably fully activated eIF4A. PTEN loss did correlate with reduced PDCD4 protein levels both in models presented herein as well as in the CCLE database and is consistent with loss of PTEN activating AKT signaling and promoting PDCD4 degradation (10). These findings suggest that PTEN mutations potentially alter the stoichiometry between eIF4A and PDCD4 by increasing the levels of eIF4A available for eIF4F complex formation and requiring higher drug levels for inhibition. It is also possible that activation of AKT stimulates additional survival pathways that result in increased resistance to eFT226. Combination of eFT226 with the PI3K/AKT inhibitors, idelalisib and MK2206, was synergistic in PTEN-mutant cell lines where AKT signaling was activated and provides rationale for combination strategies of eFT226 with select targeted agents.

The ability to target selected subgroups of patients with eFT226 would increase the likelihood of clinical benefit, improve cost-effectiveness and therapeutic outcomes. The results from this study demonstrate that the activity of eFT226 is context-dependent and a selective inhibitor of eIF4A-dependent translation is most active in the disease setting where mTOR is driving mRNA translation. This suggests that monitoring the phosphorylation level of eIF4A regulators (i.e., p70S6K, PDCD4, and eIF4G) in patient tumor samples has the potential to provide a means to subset patient populations. In addition, the association of PTEN status with eFT226 efficacy provides an additional measure that may be useful in the analysis of patient subsets during clinical development. Collectively, these findings support the clinical development of eFT226 in patients with B-cell malignancies.

Authors' Disclosures

P.A. Thompson reports other from eFFECTOR Therapeutics (employee) during the conduct of the study and is an employee or stockholder of eFFECTOR Therapeutics. G.G. Chiang reports personal fees from eFFECTOR Therapeutics (employment) during the conduct of the study. A. Gerson-Gurwitz reports other from eFFECTOR Therapeutics (employee) during the conduct of the study and is an employee or stockholder of eFFECTOR Therapeutics. S. Sperry reports other from eFFECTOR Therapeutics (employee) during the conduct of the study and has vested and unvested stock option grants in eFFECTOR Therapeutics. C. Nilewski reports a patent for US 20170145026 A1 2017-05-25 issued to eFFECTOR Therapeutic and is a stockholder and former employee of eFFECTOR Therapeutics. G.K. Packard reports a patent for US 20170145026 A1 2017-05-25 issued. T. Michels reports a patent for US 9957277B2 issued. P.A. Sprengeler reports a patent for US 9957277 and US 10577378 issued to eFFECTOR. K.R. Webster reports personal fees from eFFECTOR Therapeutics (employee) outside the submitted work. No disclosures were reported by the other authors.

Authors' Contributions

P.A. Thompson: Conceptualization, formal analysis, supervision, writing-original draft, writing-review and editing. **B. Eam:** Conceptualization, data curation, formal analysis, validation, methodology. **N.P. Young:** Conceptualization, data curation, formal analysis, validation, investigation, methodology. **S. Fish:** Conceptualization, data curation, formal analysis, validation, investigation, methodology. **J. Chen:** Data curation, software, formal analysis, validation, investigation, methodology. **M. Barrera:** Data curation, validation, investigation, methodology. **H. Howard:** Data curation, formal analysis, investigation, methodology. **E. Sung:** Data curation, formal analysis, investigation, methodology. **A. Parra:** Data curation, investigation. **J. Staunton:** Conceptualization, data curation, formal analysis, supervision, validation, investigation, methodology. **G.G. Chiang:** Conceptualization, formal analysis, supervision, methodology. **A. Gerson-Gurwitz:** Data curation. **C.J. Wegerski:** Conceptualization, data curation, formal analysis, supervision, investigation, methodology. **A. Nevarez:** Data curation, formal analysis, methodology. **J. Clarine:** Data curation, investigation, methodology. **S. Sperry:** Conceptualization, formal analysis, supervision. **A. Xiang:** Conceptualization, data curation, formal analysis, investigation, methodology. **C. Nilewski:** Conceptualization, data curation, formal analysis, investigation, methodology. **G.K. Packard:** Conceptualization, formal analysis, investigation, methodology. **T. Michels:** Conceptualization, data curation, investigation, methodology. **C. Tran:** Conceptualization, data curation, investigation, methodology. **P.A. Sprengeler:** Conceptualization, formal analysis, investigation, methodology. **J.T. Ernst:** Conceptualization, formal analysis, supervision, investigation. **S.H. Reich:** Conceptualization, supervision. **K.R. Webster:** Conceptualization, supervision, writing-original draft, writing-review and editing.

Acknowledgments

We would like to thank Amy Cortez and Yoav Altman in the flow cytometry facility, as well as SBP Medical Discovery Institute for assistance with cell sorting.

The costs of publication of this article were defrayed in part by the payment of page charges. This article must therefore be hereby marked *advertisement* in accordance with 18 U.S.C. Section 1734 solely to indicate this fact.

Received October 10, 2019; revised February 14, 2020; accepted September 30, 2020; published first October 9, 2020.

References

1. Marintchev A, Edmonds KA, Marintcheva B, Hendrickson E, Oberer M, Suzuki C, et al. Topology and regulation of the human eIF4A/4G/4H helicase complex in translation initiation. Cell 2009;136:447–60.
2. Modelska A, Turro E, Russell R, Beaton J, Sbarrato T, Spriggs K, et al. The malignant phenotype in breast cancer is driven by eIF4A1-mediated changes in the translational landscape. Cell Death Dis 2015;6:e1603.
3. Ezell SA, Wang S, Bihani T, Lai Z, Grosskurth SE, Tepsuporn S, et al. Differential regulation of mTOR signaling determines sensitivity to AKT inhibition in diffuse large B cell lymphoma. Oncotarget 2016;7:9163–74.
4. Horvilleur E, Sbarrato T, Hill K, Spriggs RV, Screen M, Goodrem PJ, et al. A role for eukaryotic initiation factor 4B overexpression in the pathogenesis of diffuse large B-cell lymphoma. Leukemia 2014;28:1092–102.
5. Parsyan A, Svitkin Y, Shahbazian D, Gkogkas C, Lasko P, Merrick WC, et al. mRNA helicases: the tacticians of translational control. Nat Rev Mol Cell Biol 2011;12:235–45.
6. Lawrence MS, Stojanov P, Mermel CH, Robinson JT, Garraway LA, Golub TR, et al. Discovery and saturation analysis of cancer genes across 21 tumor types. Nature 2014;505:495–501.

7. Suzuki C, Garces RG, Edmonds KA, Hiller S, Hyberts SG, Marintchev A, et al. PDCD4 inhibits translation initiation by binding to eIF4A using both its MA3 domains. Proc Natl Acad Sci U S A 2008;105:3274–9.
8. Dennis MD, Jefferson LS, Kimball SR. Role of p70S6K1-mediated phosphorylation of eIF4B and PDCD4 proteins in the reulgation of protein synthesis. J Biol Chem 2012;287:42890–9.
9. Ramirez-Valle F, Braunstein S, Zavadil J, Formenti SC, Schneider RJ. eIF4G1 links nutrient sensing by mTOR to cell proliferation and inhibition of autophagy. J Cell Biol 2008;181:293–307.
10. Schmid T, Jansen AP, Baker AR, Hegamyer G, Hagan JP, Colburn NH. Translation inhibitor PDCD4 is targeted for degradation dring tumor promotion. Cancer Res 2008;68:1254–60.
11. Shahbazian D, Parsyan A, Petroulakis E, Hershey J, Sonenberg N. eIF4B controls survival and proliferation and is regulated by proto-oncogenic signaling pathways. Cell Cycle 2010;9:4106–9.
12. Bhat M, Robichaud N, Hulea L, Sonenberg N, Pelletier J, Topisirovic I. Targeting the translation machinery in cancer. Nat Rev Drug Discov 2015;14: 261–78.
13. Ernst JT, Reich SH, Sprengeler PA, Tran CV, Packard GK, Xiang AX, et al. inventors; Effector Therapeutics, assignee. eIF4A-inhibiting compounds and methods related thereto. United States patent US 20170145026 A1. 2017 May 25.
14. Hirai H, Sootome H, Nakatsuru Y, Miyama K, Taguchi S, Tsujioka K, et al. MK-2206, an allosteric AKT inhibitor, enhances antitumor efficacy by standard chemotherapeutic agents or molecular targetd drugs in vitro and in vivo. Mol Cancer Ther 2010;9:1956–67.
15. Chou TC, Talalay P. Analysis of combine drug effects: a new look at a very old problem. Trends Pharmacol Sci 1983;4:450–4.
16. Dorrello NV, Peschiaroli A, Guardavaccaro D, Colburn NH, Sherman NE, Pagano M. S6K1- and βTRCP-mediated degradation of PDCD4 promotes protein translation and cell growth. Science 2006;314: 467–71.
17. Galan JA, Geraghty KM, Lavoie G, Kanshin E, Tcherkezian J, Calabrese V, et al. Phosphoproteomic analysis identifies the tumor suppressor PDCD4 as a RSK substrate negatively regulated by 14-3-3. Proc Nat Acad Sci U S A 2014;111: E2918–27.
18. Hsieh AC, Ruggero D. Targeting eukaryotic translation initiation factor 4E (eIF4E) in cancer. Clin Cancer Res 2010;16:4914–20.
19. Steinhardt JJ, Peroutka RJ, Mazan-Mamczarz K, Chen Q, Houng S, Robles C, et al. Inhibiting CARD11 translation during BCR activation by targeting the eIF4A RNA helicase. Blood 2014;124:3758–67.
20. Zhang X, Bi C, Lu T, Zhang W, Yue T, Wang C, et al. Targeting translation initiation by synthetic rocaglates for treating MYC-driven lymphomas. Leukemia 2019;34:138–50.
21. Ernst JT, Thompson PA, Nilewski C, Sprengeler PA, Sperry S, Packard G, et al. Design of development candidate eFT226, a first in class inhibitor of eukaryotic initiation factor 4A RNA helicase. J Med Chem 2020;63:5879–955.
22. Iwasaki S, Floor SN, Ingolia NT. Rocaglates convert DEAD-box protein eIF4A into a sequence-selective translational repressor. Nature 2016;534:558–61.
23. Sadlish H, Galicia-Vazquez G, Paris CG, Aust T, Bhullar B, Chang L, et al. Evidence for a functionally relevant rocaglamide binding site on the eIF4A-RNA complex. Chem Biol 2013;8:1519–27.
24. Chu J, Galicia-Vazquez G, Cencic R, Mills JR, Katigbak A, Porco JA, et al. CRISPR-mediated drug-target validation reveals selective pharmacological inhibitionof the RNA helicase, eIF4A. Cell Rep 2016;15:1–8.
25. Iwasaki S, Iwasaki W, Takahashi M, Sakamoto A, Watanabe C, Shichino Y, et al. The translation inhibitor Rocaglamide targets a biomolecular cavity between eIF4A and polypurine RNA. Mol Cell 2019;73:1–11.
26. Wolfe AL, Singh K, Zhong Y, Drewe P, Rajasekhar VK Sanghvi VR, et al. RNA G-quadruplexes cause eIF4A dependent oncogene translation in cancer. Nature 2014;513:65–70.
27. Rubio CA, Weisburd B, Holderfield M, Arias C, Fang E, DeRisi JL, et al. Transcriptome-wide characterization of the eIF4A signature highlights plasticity in translation regulation. Genome Biol 2014;15:1–19.
28. Manier S, Huynh D, Shen YJ, Zhou J, Yusufzai T, Salem KZ, et al. Inhibiting the oncogenic translation program is an effective therapeutic strategy in multiple myeloma. Sci Transl Med 2017;9:eaal2668.
29. Maurer U, Charvet C, Wagman AS, Dejardin E, Green DR. Glycogen synthase kinase-3 regulates mitochondrial outer membrane permeabilization and apoptosis by destabilization of MCL-1. Mol Cell 2006;21:749–60.
30. Brunelle JK, Ryan J, Yecies D, Opferman JT, Letai A. MCL-1 dependent leukemia cells are more sensitive to chemotherapy than BCL-2-dependent counterparts. J Cell Biol 2009;187:429–42.
31. Johnson JI, Decker S, Zaharevitz D, Rubinstein LV, Venditti JM, Schepartz S, et al. Relationships between drug activity in NCI preclinical in vitro and in vivo models and early clinical trials. Brit J Can 2001;84:1424–31.